Optimum signal-to-noise ratio in off-axis integrated cavity output spectroscopy

Christoph Dyroff

Karlsruhe Institute of Technology, Institute of Meteorology and Climate Research, Hermann-von-Helmholtz-Platz 1, 76344 Eggenstein-Leopoldshafen, Germany (christoph.dyroff@kit.edu)

Received December 23, 2010; revised February 10, 2011; accepted February 22, 2011; posted February 24, 2011 (Doc. ID 140047); published March 22, 2011

The signal-to-noise ratio (SNR) in off-axis integrated cavity output spectroscopy (OA-ICOS) is investigated and compared to direct absorption spectroscopy using multipass absorption cells [tunable diode laser absorption spectroscopy (TDLAS)]. Applying measured noise characteristics of a near-IR tunable diode laser and detector, it is shown that the optimum SNR is not generally reached at the highest effective absorption path length. Simulations are used to determine the parameters for maximized SNR of OA-ICOS.

OCIS codes: 300.6360, 120.6200, 270.2500.

It often appears to be the consensus that the longer the optical path in a laser-absorption experiment, the higher the sensitivity [1–3]. Indeed, from the Beer–Lambert-law point of view this seems justified. The classical approach to path length enhancement is the use of multipass absorption cells (MPCs) [4,5]. There, the laser beam enters the MPC through a hole in the front mirror and, after being reflected N times, generally exits the MPC through the same hole (at an inverted angle) when fulfilling the reentrant condition. For a large volume MPC, Richard *et al.* [6] have achieved 252 m path length with $N = 454$. In smaller volume cells, the maximum number of passes is usually lower, such as $N = 238$ and 76 m path length for the commercially available AMAC-76 (Aerodyne Research, Inc., USA).

Cavity-enhanced absorption techniques have gained attention due to their potential to achieve very long effective optical path lengths of up to several kilometers [1,3,7–9]. Off-axis integrated cavity output spectroscopy (OA-ICOS) is a particularly interesting approach due to its mechanical robustness and relatively simple alignment [1,9]. In an OA-ICOS experiment two spherical (or slightly astigmatic) mirrors with high reflectivity, R, are aligned *vis-à-vis* to form an optical resonator of base length L. The laser beam with optical power $\overline{P_0}$ (the bar denotes an average value) is injected into the cavity through one of the mirrors in an off-axis alignment. Inside the cavity, a high number of cavity modes is excited, and, similar to multipass cells, the spots on the mirrors either form a circle (spherical mirrors) or a Lissajous pattern (astigmatic mirrors) [10]. This reduces the free spectral range (FSR) of the cavity proportional to the number of excited cavity modes. Then, the spectral linewidth of the laser is much larger than the cavity FSR, and the transmission spectrum of the empty cavity becomes a continuum, i.e., the cavity is assumed to be nonresonant. The laser radiation leaking out of the rear mirror is collected and focused onto a detector to record the cavity transmission.

By discussing electronic and photon noise defining the signal-to-noise ratio (SNR), two findings will be shown: (1) the highest SNR is not generally achieved at the highest effective path length, a fact that has only briefly been discussed before [9]; (2) similar limits of detection may be achieved with much shorter path lengths using tunable diode laser absorption spectroscopy (TDLAS).

The effective optical path length, l, in OA-ICOS is the product of the cavity-base length, L, and the gain factor, $G = 1/(1 - R)$, i.e., $l = LG$ [9]. Assuming the cavity to be in steady state, the optical power at the detector in the absence of an absorber is $\overline{P_{\mathrm{opt}}} = \overline{P_0} T_M C_p/(2G)$ [1]. Here the factor 2 accounts for laser radiation leaking out through both cavity mirrors; T_M is the mirror transmission (0…1), and C_p is a spatial coupling parameter (0…1) [1]. In the presence of an absorber with single-pass absorption, $A(\nu_0) = 1 - \exp[-\alpha(\nu_0)L]$, the absorbed power at the absorption line center is [11]

$$\overline{P_A(\nu_0)} = \frac{\overline{P_0} T_M C_p}{2} \cdot \frac{1}{G + 1/A(\nu_0)}. \quad (1)$$

An equivalent description can be made for a TDLAS experiment using a two-mirror MPC [12]. With mirror reflectivity R and base length L, the power on the detector after N passes in the absence of an absorber is $\overline{P_{\mathrm{opt}}} = \overline{P_0} R^{(N-1)}$. According to the Beer–Lambert law, in the presence of an absorber the absorbed power at line center is

$$\overline{P_A(\nu_0)} = \overline{P_0} R^{(N-1)} \{1 - \exp[-\alpha(\nu_0) N L]\}. \quad (2)$$

In both cases the transmitted optical power at line center is $\overline{P_T(\nu_0)} = \overline{P_{\mathrm{opt}}} - \overline{P_A(\nu_0)}$.

The noise in any photon-detection system, here quantified as variance of the power fluctuations, $\overline{\delta P^2}$, at the detector in a certain measurement bandwidth, Δf, can be described by three contributions [13]. (1) Dark noise, $\overline{\delta P^2_{\mathrm{dark}}} \Delta f$, of the detector, preamplifier, and subsequent electronics, which is due to e.g., the thermal noise of resistors, the noise of the detector dark current, as well as noise from the preamplifier power supply. (2) Shot noise, $\overline{\delta P^2_{\mathrm{shot}}} = 2eS^{-1} \overline{P_{\mathrm{opt}}} \Delta f$, with $e = 1.602 \times 10^{-19}\,\mathrm{C}$, the detector responsivity S, and the optical power $\overline{P_{\mathrm{opt}}}$ at the detector. It is the lowest possible noise level for photon detection. (3) Lasers show additional intensity fluctuations (excess noise) quantified as relative-intensity noise (RIN), $\mathrm{RIN} = \overline{\delta P^2_{\mathrm{excess}}}/(\overline{P_{\mathrm{opt}}}^2 \Delta f)$, which is due to

0146-9592/11/071110-03$15.00/0

(amplified) spontaneous emission of photons as well as laser-mode competition.

The variance of all three contributions is added to the total noise variance $\overline{\delta P^2}$. In the presence of an absorber, $\overline{P_{\mathrm{opt}}}$ is replaced by $\overline{P_T}$, and $\overline{\delta P^2}$ can be expressed as [14]

$$\overline{\delta P^2} = \overline{\delta P^2_{\mathrm{dark}}}\Delta f + 2eS^{-1}\overline{P_T}\Delta f + \mathrm{RIN}\overline{P_T}^2\Delta f. \quad (3)$$

An OA-ICOS cavity can be thought of as a low-pass filter for (fast) optical fluctuations originating from the laser source. The 3 dB bandwidth of the cavity is $\Delta f_{\mathrm{cavity}} = 1/(2\pi\tau_{\mathrm{RD}})$ [1], where $\tau_{\mathrm{RD}} = l/c$ is the characteristic cavity ringdown time. Thus, for OA-ICOS, RIN has to be considered in the $\Delta f_{\mathrm{cavity}}$ bandwidth if $\Delta f_{\mathrm{cavity}} < \Delta f$.

The SNR for a laser spectrometer is defined as the ratio of absorption signal and noise

$$\mathrm{SNR} = \frac{\overline{P_A}}{\sqrt{\overline{\delta P^2}}}. \quad (4)$$

For its quantification, noise measurements were carried out using the setup depicted in Fig. 1(a). A constant laser-injection current, I_{LD}, was provided by a low-noise laser driver (ITC102, Thorlabs, Inc., USA) to a fiber-pigtailed distributed-feedback laser diode (LD) emitting at $\nu_0 = 7184\,\mathrm{cm}^{-1}$ ($\lambda_0 = 1.392\,\mu\mathrm{m}$) (NLK1E5E1AA, NTT Electronics, Japan). At $I_{\mathrm{LD}} = 120\,\mathrm{mA}$ and $T_{\mathrm{LD}} = 25\,°\mathrm{C}$, $\overline{P_0} = 20\,\mathrm{mW}$ was measured. The uncollimated laser beam was guided onto an InGaAs photodiode (PD) fitted with a transimpedance amplifier (TIA) (PDA400, Thorlabs, Inc., USA, $S = 0.88\,\mathrm{A/W}$, $R_F = 1.5 \times 10^4\,\mathrm{V/A}$, $\Delta f = 10\,\mathrm{MHz}$), and $\overline{P_{\mathrm{opt}}}$ was measured at various distances, d, between fiber tip and PD. The optical power at the detector was inferred from the measured voltage (DC component $\overline{U}$, AC component u_{rms}) at the output of

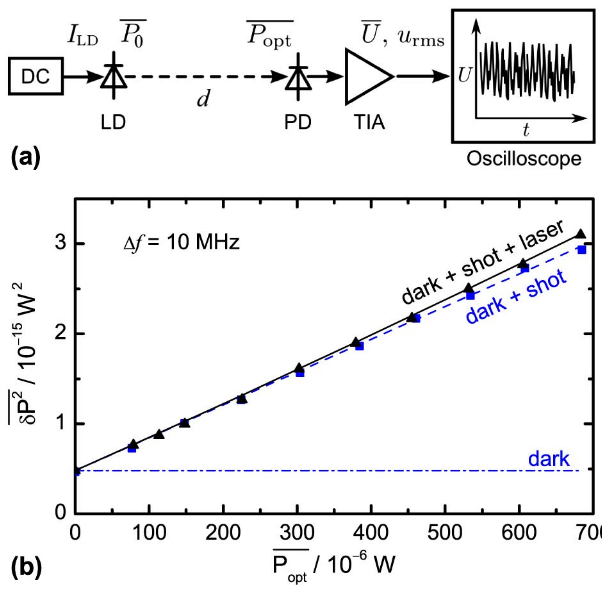

Fig. 1. (Color online) (a) Constant injection current, I_{LD}, is provided to the LD. $\overline{P_{\mathrm{opt}}}$ is detected by a PD. Mean voltage $\overline{U}$ and fluctuation u_{rms} are measured by an oscilloscope at the output of a TIA. (b) Variance of noise power ($\overline{\delta P^2}$) as a function of mean optical power ($\overline{P_{\mathrm{opt}}}$) showing dark noise, shot noise, and laser excess noise contributions.

the TIA using its feedback resistance, R_{F}, and the detector responsivity, S by $P = U/(R_{\mathrm{F}}S)$.

Figure 1(b) depicts the measured optical noise variance $\overline{\delta P^2}$ with respect to $\overline{P_{\mathrm{opt}}}$. $\overline{\delta P^2_{\mathrm{dark}}}\Delta f = 4.83 \times 10^{-16}\,\mathrm{W}^2$ (horizontal line) was measured with the detector active area blocked, corresponding to a noise-equivalent power (NEP) of $\mathrm{NEP} = 6.95 \times 10^{-12}\,\mathrm{WHz}^{-1/2}$, which is in good agreement with the specifications ($8.2 \times 10^{-12}\,\mathrm{WHz}^{-1/2}$). The shot noise level (dashed line, calculated; squares, measured) was measured using a thermal light source (light bulb) that does not show excess noise [13]. The black triangles show measurements for the laser. A fit (black line) of the measured data to Eq. (3) yields $\mathrm{RIN} = 3 \times 10^{-17}\,\mathrm{Hz}^{-1}$, measured in $\Delta f = 10\,\mathrm{MHz}$.

A model for the SNR in both OA-ICOS and TDLAS was derived based on Eqs. (1)–(4). Therein, the baselength of both the OA-ICOS cavity and the MPC is $L = 0.3\,\mathrm{m}$, and the single-pass absorption is set to $A(\nu_0) = 1 \times 10^{-5}$. Probing a water ($H_2O$) absorption line at $\nu_0 = 7183.685\,\mathrm{cm}^{-1}$, this corresponds to a volume-mixing ratio of ≈20 ppmv at a gas pressure of 50 hPa and a temperature of 30 °C. The laser output power is again $\overline{P_0} = 20\,\mathrm{mW}$. For OA-ICOS, both $T_M = 1$ and $C_P = 1$ is assumed. In the calculations, the mirror reflectivity, R, is varied, leading to a variation of effective optical path length and transmitted power on the detector. For TDLAS, $R = 0.99$ (dielectric coating) is assumed, and N is varied to achieve different path lengths. As with OA-ICOS, ideal coupling of the laser beam to the MPC is assumed for TDLAS.

Figure 2 depicts the calculated SNR using the measured specifications of the near-IR laser and PDA400 (Thorlabs, Inc.) detector for OA-ICOS (solid line 1) and TDLAS (dashed line 2). For both techniques, the SNR is increased with increasing absorption path length, l, until a certain maximum ($\mathrm{SNR}_{\mathrm{max}}$) is reached. Because of the relatively high power incident on the detector for TDLAS, $\overline{P_{\mathrm{opt}}}$ at the maximum SNR is attenuated to 90% of the full-scale specification of the detector to avoid saturation. The increase in SNR for OA-ICOS is explained as follows: the fractional absorption is enhanced with increasing path length. Despite a reduction of $\overline{P_{\mathrm{opt}}}$ incident on the detector, this yields a constant $\overline{P_A}$. Furthermore,

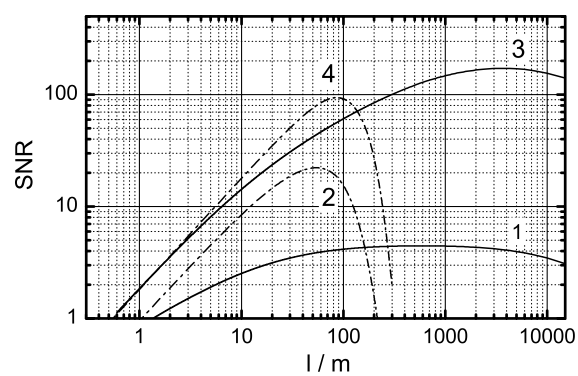

Fig. 2. Calculated SNR. OA-ICOS, solid lines 1 (PDA400) and 3 (PDA10DT) for $\overline{P_0} = 20\,\mathrm{mW}$, single-pass absorption $A(\nu_0) = 1 \times 10^{-5}$, $L = 0.3\,\mathrm{m}$, $T_M = 1$, $C_P = 1$. TDLAS, dashed lines 2 (PDA400) and 4 (PDA10DT) for $R = 0.99$.

$\overline{\delta P^2}$ is reduced due to the lower $\overline{P_T}$ at increasing l [Eq. (3)]. The steeper increase in SNR for TDLAS is due to the increase in $\overline{P_A}$ with increasing l. In both cases, increasing l beyond the optimum reduces the SNR, because then $\overline{P_A}$ is reduced. For high l, $\overline{\delta P^2}$ becomes practically constant ($\overline{\delta P^2_{\rm dark}}\Delta f$).

For OA-ICOS (solid line 1), $\mathrm{SNR}_{\rm max} = 4.5$ is reached at $l \approx 590\,\mathrm{m}$ ($R = 0.99949$, $\overline{P_{\rm opt}} = 5.1\,\mu\mathrm{W}$). Correspondingly, $\mathrm{SNR}_{\rm max} = 22$ is determined at $l = 54\,\mathrm{m}$ ($N = 180$, attenuated $\overline{P_{\rm opt}} = 682\,\mu\mathrm{W}$) for TDLAS. Despite the ≈11× shorter path length, TDLAS yields a ≈5× higher SNR.

For comparison, a thermoelectrically cooled InGaAs detector with TIA providing both lower NEP and Δf (Thorlabs PDA10DT, $S = 0.5\,\mathrm{A/W}$, $R_F = 1.51 \times 10^5\,\mathrm{V/A}$, $\mathrm{NEP} = 1.37 \times 10^{-12}\,\mathrm{WHz}^{-1/2}$, $\Delta f = 115\,\mathrm{kHz}$) was assumed. For OA-ICOS (solid line 3) the SNR is increased 35× to $\mathrm{SNR}_{\rm max} = 172$, and it is reached at $l = 3750\,\mathrm{m}$ ($R = 0.99992$, $\overline{P_{\rm opt}} = 0.8\,\mu\mathrm{W}$). Using mirrors with higher reflectivity to enhance the effective path length would be counterproductive, unless a detector/TIA with lower NEP is available. For TDLAS (dashed line 4), $\mathrm{SNR}_{\rm max} = 94$ (4× enhancement) is achieved at $l = 86\,\mathrm{m}$ ($N = 286$, attenuated $\overline{P_{\rm opt}} = 119\,\mu\mathrm{W}$). For this system configuration, $\mathrm{SNR}_{\rm max}$ is ≈2× higher for OA-ICOS than for TDLAS. The lower increase in SNR for TDLAS is due to the lower contribution of $\overline{\delta P^2_{\rm dark}}$ to the total noise when compared to OA-ICOS.

The results presented are only valid for the configurations discussed, because they are based on specific noise characteristics. However, the methods provided are straightforward and can readily be applied to any other configuration.

It should be pointed out that the overall performance of a spectrometer, independent of the technique used, also depends on additional limiting effects. In practice, OA-ICOS mirrors have slight absorptive losses ($T_M < 1$), and the setup may show imperfect spatial coupling ($C_p < 1$), e.g., when only a fraction of the laser radiation can be focused on the detector [9]. Both effects reduce the power incident on the detector and thus SNR. Also, unwanted time-dependent interference structures superimposed on the measured spectra or the quality of the fit algorithm may affect the performance of a laser spectrometer, because signal averaging may not effectively enhance SNR due to systematic drift [9,15].

Especially in the mid-IR spectral region, detectors show higher NEP [9], which reduces the SNR of OA-ICOS to a greater extent than that of TDLAS. On the other hand, mid-IR lasers such as quantum-cascade lasers may reveal higher RIN [16,17], which plays a more important role in TDLAS. Given a similar RIN, higher laser power will enhance the SNR more in OA-ICOS than in TDLAS.

References

1. J. B. Paul, L. Lapson, and J. G. Anderson, Appl. Opt. **40**, 4904 (2001).
2. L. Menzel, A. A. Kosterev, R. F. Curl, F. K. Tittel, C. Gmachl, F. Capasso, D. L. Sivco, J. N. Baillargeon, A. L. Hutchinson, A. Y. Cho, and W. Urban, Appl. Phys. B **72**, 859 (2001).
3. D. S. Baer, J. B. Paul, M. Gupta, and A. O'Keefe, Appl. Phys. B **75**, 261 (2002).
4. D. Herriott, H. Kogelnik, and R. Kompfner, Appl. Opt. **3**, 523 (1964).
5. J. B. McManus, P. L. Kebabian, and M. S. Zahniser, Appl. Opt. **34**, 3336 (1995).
6. E. C. Richard, K. K. Kelly, R. H. Winkler, R. Wilson, T. L. Thompson, R. J. McLaughlin, A. L. Schmeltekopf, and A. F. Tuck, Appl. Phys. B **75**, 183 (2002).
7. A. O'Keefe and A. G. Deacon, Rev. Sci. Instrum. **59**, 2544 (1988).
8. A. O'Keefe, J. J. Scherer, and J. B. Paul, Chem. Phys. Lett. **307**, 343 (1999).
9. E. J. Moyer, D. S. Sayres, G. S. Engel, J. M. St. Clair, F. N. Keutsch, N. T. Allen, J. H. Kroll, and J. G. Anderson, Appl. Phys. B **92**, 467 (2008).
10. D. S. Sayres, E. J. Moyer, T. F. Hanisco, J. M. S. Clair, F. N. Keutsch, A. O'Brien, N. T. Allen, L. Lapson, J. N. Demusz, M. Rivero, T. Martin, M. Greenberg, C. Tuozzolo, G. S. Engel, J. H. Kroll, J. B. Paul, and J. G. Anderson, Rev. Sci. Instrum. **80**, 044102 (2009).
11. Y. A. Bakhirkin, A. A. Kosterev, C. Roller, R. F. Curl, and F. K. Tittel, Appl. Opt. **43**, 2257 (2004).
12. P. Werle and F. Slemr, Appl. Opt. **30**, 430 (1991).
13. E. L. Dereniak and G. D. Boreman, *Infrared Detectors and Systems* (Wiley, 1996).
14. H. Fischer and M. Tacke, J. Opt. Soc. Am. B **8**, 1824 (1991).
15. P. Werle, P. Mazzinghi, F. D'Amato, M. D. Rosa, K. Maurer, and F. Slemr, Spectrochim. Acta, Part A **60**, 1685 (2004).
16. T. Gensty, W. Elsässer, and C. Mann, Opt. Express **13**, 2032 (2005).
17. Y. Takagi, N. Kumazaki, M. Ishihara, K. Kasahara, A. Sugiyama, N. Akikusa, and T. Edamura, Electron. Lett. **44**, 860 (2008).